JOURNAL OF VIROLOGY, Mar. 1999, p. 1774–1784 Vol. 73, No. 3
0022-538X/99/$04.00+0

Severe Leukopenia and Dysregulated Erythropoiesis in SCID Mice Persistently Infected with the Parvovirus Minute Virus of Mice

JOSÉ C. SEGOVIA,[1] JESÚS M. GALLEGO,[2] JUAN A. BUEREN,[1] AND JOSÉ M. ALMENDRAL[2]*

Departamento de Biología Molecular y Celular, CIEMAT, 28040 Madrid,[1] and Centro de Biología Molecular "Severo Ochoa," Universidad Autónoma de Madrid, 28049 Cantoblanco, Madrid,[2] Spain

Received 10 August 1998/Accepted 12 November 1998

Parvovirus minute virus of mice strain i (MVMi) infects committed granulocyte-macrophage CFU and erythroid burst-forming unit (CFU-GM and BFU-E, respectively) and pluripotent (CFU-S) mouse hematopoietic progenitors in vitro. To study the effects of MVMi infection on mouse hemopoiesis in the absence of a specific immune response, adult SCID mice were inoculated by the natural intranasal route of infection and monitored for hematopoietic and viral multiplication parameters. Infected animals developed a very severe viral-dose-dependent leukopenia by 30 days postinfection (d.p.i.) that led to death within 100 days, even though the number of circulating platelets and erythrocytes remained unaltered throughout the disease. In the bone marrow of every lethally inoculated mouse, a deep suppression of CFU-GM and BFU-E clonogenic progenitors occurring during the 20- to 35-d.p.i. interval corresponded with the maximal MVMi production, as determined by the accumulation of virus DNA replicative intermediates and the yield of infectious virus. Viral productive infection was limited to a small subset of primitive cells expressing the major replicative viral antigen (NS-1 protein), the numbers of which declined with the disease. However, the infection induced a sharp and lasting unbalance of the marrow hemopoiesis, denoted by a marked depletion of granulomacrophagic cells (GR-1$^+$ and MAC-1$^+$) concomitant with a twofold absolute increase in erythroid cells (TER-119$^+$). A stimulated definitive erythropoiesis in the infected mice was further evidenced by a 12-fold increase per femur of recognizable proerythroblasts, a quantitative apoptosis confined to uninfected TER-119$^+$ cells, as well as by a 4-fold elevation in the number of circulating reticulocytes. Therefore, MVMi targets and suppresses primitive hemopoietic progenitors leading to a very severe leukopenia, but compensatory mechanisms are mounted specifically by the erythroid lineage that maintain an effective erythropoiesis. The results show that infection of SCID mice with the parvovirus MVMi causes a novel dysregulation of murine hemopoiesis in vivo.

The hemopoietic system displays a wide repertoire of proliferating cells at diverse differentiation and commitment stages generated from a small group of pluripotent stem cells (50). The tight control of this development is exerted by a network of signaling pathways onset by cellular interactions and growth factors binding to their cognate receptors (reviewed in references 21, 39, and 55). Many viral infections are accompanied by the perturbation of hemopoiesis homeostasis (72, 70). The complexity of mechanisms underlying these alterations extends from the direct action of virus-coded effectors to the concourse of host regulatory factors.

The infection of viruses belonging to the *Parvoviridae* family is commonly associated with hematological diseases. This family includes a large group of small viruses containing a linear single-stranded (ss) DNA genome with a nonenveloped 25-nm-diameter icosahedral capsid (57). The genome encodes nonstructural (NS1 and NS2) and structural proteins (VP1 and VP2) that form parvovirus particles. The major nonstructural protein NS1 is essential for replication and packaging of the viral genome (4, 17, 52) and transcriptional activity (22, 23) and is toxic to the host cell (15, 37, 42); therefore, its expression is a major indication of permissive parvoviral infection. A general feature of parvoviruses multiplication is the requirement for functions expressed during the S phase of the cell cycle (5, 61, 63). This explains why a common characteristic in the pathogenesis of these viruses is the infection of mitotically active cells and why clinical courses are more severe in developing hosts with many tissues undergoing proliferation (56, 59).

Parvovirus tropism is also constrained by factors expressed at certain differentiation stages (40, 58, 62). In fact, the target cell specificity differs among the parvoviruses, and therefore their infections are accompanied by characteristic alterations of the lymphohemopoietic system. Aleutian mink disease parvovirus (ADV) causes a persistent infection with severe disorders of the immune system of this animal (43, 48). Experimental and natural infections with the feline panleukopenia virus develops neutropenia in cats (34–36). The parvovirus B19 is the only known member of the *Parvoviridae* that is pathogenic to humans (65, 71). The virus shows a selective tropism for hemopoietic precursors of the erythroid lineage (28, 44), interacting for the infection with the glycolipid globoside of the blood group P antigens that acts as a receptor of the virus (13, 16). The B19 is the etiological agent of a childhood measles-like rash called "erythema infectiosum" or fifth disease (1), and its intranasal inoculation into volunteers caused transient changes in the reticulocyte and hemoglobin (2) counts and a reduction in peripheral and marrow erythroid precursors 10 days postinoculation at the time of viremia (49). In patients with hemoglobinopathies, an acute B19 infection results in transient aplastic crisis because of the abrupt cessation of erythrocyte production (47), and the virus infection is manifested by the appearance of early erythroid cells or giant

* Corresponding author. Mailing address: Centro de Biología Molecular "Severo Ochoa," Universidad Autónoma de Madrid, 28049 Cantoblanco, Madrid, Spain. Phone: 34-913978048. Fax: 34-913978087. E-mail: jmalmendral@cbm.uam.es.

TABLE 1. Hematologic and erythrocytic values for mock- and MVMi-infected adult SCID mice[a]

Mouse group	RBC (10^6/μl)	Hgb (g/dl)	Hct (%)	MCV (fl)	MCH (pg)	MCHC (g/dl)
Mock infected	9.77 ± 0.87	15.50 ± 0.54	41.60 ± 4.34	42.51 ± 1.32	15.93 ± 1.00	37.50 ± 3.01
MVMi infected	8.76 ± 0.77*	13.72 ± 1.16**	37.94 ± 3.26	41.46 ± 1.31	15.69 ± 1.23	37.85 ± 2.37

[a] Values indicate the mean ± the standard error of the mean ($n = 8$ animals in each group). *, $P < 0.05$; **, $P < 0.01$ (t test). Abbreviations: RBC, erythrocytes; Hgb, hemoglobin concentration; Hct, hematocrit; MCV, mean corpuscular volume; HCM, mean corpuscular hemoglobin content; MCHC, mean corpuscular hemoglobin concentration.

pronormoblasts in the marrow (45, 46). In pregnant women infection may cause hydrops fetalis and spontaneous abortion due to the inability of the fetus to mount an adequate immune response. In immunocompromised individuals, such as patients with AIDS or patients undergoing immunosuppressive drug therapy, the persistent B19 infection causes an erythroid marrow failure with chronic severe anemia (27, 33).

Among the rodent parvoviruses (64), the i strain of the parvovirus minute virus of mice (MVMi) suppresses in vitro both a number of T-lymphocyte functions (9, 24), as well as the clonogenic capacity of different hemopoietic precursors, and it is able to efficiently multiply in primary myeloid cultures (53). After intranasal inoculation of newborn mice, the MVMi at a low viral dose spread to many organs and induced a runting syndrome (31), but at a high viral dose it caused a lethal infection in some inbred strains of mice, an infection whose histopathological hallmarks are renal papillary hemorrhage and involution of hepatic erythropoietic foci (14), hypocellularity at germinal centers in mouse postbirth neurogenesis (51), and a temporal myeloid depression in the bone marrow and spleen that is soon restricted by an early humoral immune response (54). The complexity of MVMi pathogenesis in the newborn mouse makes this an inadequate model to evaluate the MVMi hemopoietic pathogenic potential in vivo.

This study focused on the interaction of MVMi with mouse hemopoiesis in the adult mouse with the severe combined immunodeficiency mutation (SCID [11]) to avoid both an antigen-specific immune response and the viral multiplication in the developing tissues of the newborn. The SCID mice lack functional B and T cells, but the myeloid and erythroid lineages are unaffected (3, 11). We have determined an unexpected capacity of the MVMi to unbalance the ratio of the granulomacrophage versus the erythroid lineage of adult SCID mice. Animals persistently infected by MVMi developed leukopenia but not anemia, although the virus deeply suppressed clonogenic progenitors of both lineages. The analysis of the mechanisms underlying this unprecedented infectious disease has revealed a specific capacity of the erythropoiesis to functionally compensate a viral depletion of early hemopoietic progenitors.

MATERIALS AND METHODS

Virus and cell lines. MVMi was prepared by low-multiplicity infection of the EL-4 mouse C57BL T-cell lymphoma line. As inocula to infect the mice, we employed purified virus banded in density gradients (53) that was further sterile filtered (0.22 μm) before titration. Virus titers were determined by plaque assay on the NB324K human simian virus 40-transformed newborn kidney cells as described previously (51). To visualize the plaques, monolayers were fixed overnight with 10% formaldehyde and stained with 0.2% crystal violet. The origin of our virus strain and the cell lines to handle it have been previously described (53). Cells were cultured in Dulbecco modified Eagle medium (GIBCO Laboratories, Grand Island, N.Y.) supplemented with 5% inactivated fetal bovine serum (FBS).

Mice and virus infection. The severe combined immunodeficient C.B-17 inbred strain of SCID mice was originally purchased from the Jackson Laboratories (Bar Harbor, Maine) and subsequently bred in our animal facility (Centro de Biología Molecular Severo Ochoa, Madrid, Spain) that is screened regularly for mouse pathogens, including rodent parvoviruses. Mice were maintained in isolated cabinets under sterile air flow (IFFA-CREDO) under a 12-h light-dark cycle housed in sterile microisolator cages and were given autoclaved food and water ad libitum. Mouse handling was done according to European Union guidelines (86/609/CEE). For the infections, 8- to 10-week-old female mice homozygous for the *scid* mutation were intranasally inoculated with purified virus in phosphate-buffered saline (PBS) in a constant volume of 10 μl. Mice were anesthetized with ether for best inhalation of the inocula. Mock-infected mice received the same volume of PBS. Infected mice were monitored for the leaky antibody production characteristic of the SCID phenotype (10), and in no case was a specific anti-MVM capsid immunoglobulin synthesis detected by an enzyme-linked immunosorbent assay (ELISA) test (54).

Peripheral blood parameters. Blood samples (50 to 100 μl) were obtained by a small incision in the lateral tail vein of mice previously heated under a 100-W lamp for 5 min. Blood was collected on tubes containing a final concentration of 20 mM EDTA to avoid coagulation, and aliquots were appropriately diluted on Turk solution (2% acetic acid, 0.01% methylene blue), 1% ammonium oxalate, or PBS to count leukocytes (WBC), platelets, or erythrocytes, respectively. The cell numbers were determined by duplicate counting in a hemocytometer. When mice were monitored for several weeks, only 10 μl of blood for the analysis of WBC was extracted. The erythroid indices shown in Table 1 were determined with an automated hematology analyzer (Technicon H.1E; Bayer) with the parameters selected for mouse peripheral blood. The level of significance of the differences between groups was determined by using the two-tailed Student's t test evaluated by the SPSS software, version 6.1.2 (SPSS, Inc.).

Blood and marrow cell staining. Blood smears or Cytospin (Shandon Southern Products, Cheshire, United Kingdom)-centrifuged bone marrow cells were fixed with methanol and stained by the May-Grünwald-Giemsa standard technique. Cellular samples were morphologically studied under a microscope, and the classification of marrow cell populations outlined in Fig. 7 was verified by an external service (Department of Pathology and Infectious Diseases, Royal Veterinary College, London, United Kingdom). For reticulocyte evaluation, blood films were incubated for 20 min at room temperature with 1 volume of Cresil Blue prior to the staining. Preparations were observed and photographed on a Zeiss Axiophot microscope.

Bone marrow cells and progenitor clonogenic assays. Bone marrow cells from each infected or uninfected mouse were obtained by flushing Iscove's modified Dulbecco medium (IMDM; GIBCO) through the shaft of individually dissected femora and tibiae. Cells were dispersed with a 16- by 5-mm needle and washed three times in IMDM, and the number of nucleated cells was determined after triplicate counting in a hemocytometer. When indicated, bone marrow cell viability was assessed by Trypan blue exclusion. Hemopoietic progenitors were assessed in enriched methylcellulose semisolid cultures essentially as described earlier (53). The culture medium consisted of IMDM, 30% FBS, 1% deionized bovine serum albumin (BSA; fraction V; Sigma Chemical Co., St. Louis, Mo.), 10% conditioned medium of the cell line WEHI-3b, 0.8% methylcellulose (Dow Chemical Co., Midland, Mich.), 2 U of erythropoietin per ml (Therry Fox Laboratory, Vancouver, British Columbia, Canada), 10^{-2} mM α-thioglycerol, 2×10^{-3} mM L-glutamine, and 10^{-4} mM Na_2SeO_3. A fixed number of 10^5 nucleated cells resuspended in a final volume of 0.9 ml of medium were dispensed in three wells of a 24-well culture dish (Nunc, Roskilde, Denmark), and colonies were scored under an inverted microscope after 7 days incubation in a fully humidified atmosphere of 5% CO_2 at 37°C. Progenitors from uninfected mice were always assayed in parallel in the same dishes as an internal control for the cultures. Granulocyte-macrophage colony-forming units (CFU-GM) were defined as aggregates of at least 50 cells, and burst-forming unit erythroid colonies (BFU-E) were defined as hemoglobinized bursts.

Flow cytometry analysis. Bone marrow cells were washed and resuspended at 10^7 cells/ml in PBA (PBS, 0.1% BSA, 0.02% sodium azide). Next, 100-μl cell suspensions were incubated for 30 min at 4°C with GR-1-FITC, MAC-1-FITC, and TER-119-PE antibodies (PharMingen, San Diego, Calif.) or a purified monoclonal raised against the NS-1 protein of MVM (kindly provided by C. A. Astell, Vancouver, British Columbia, Canada) upon cell permeabilization as described earlier (69). Thereafter, erythrocytes were lysed by adding 2.5 ml of lysis solution (0.155 M NH_4CL, 0.01 M $KHCO_3$, 0.1 mM EDTA); the suspensions were then incubated at room temperature for 5 min and washed with PBA. To study apoptotic cell death, the DNA fragmentation of the cells was determined after propidium iodide (PI) staining of the samples without any previous permeabilization step (32). Cell parameters were analyzed with an EPICS

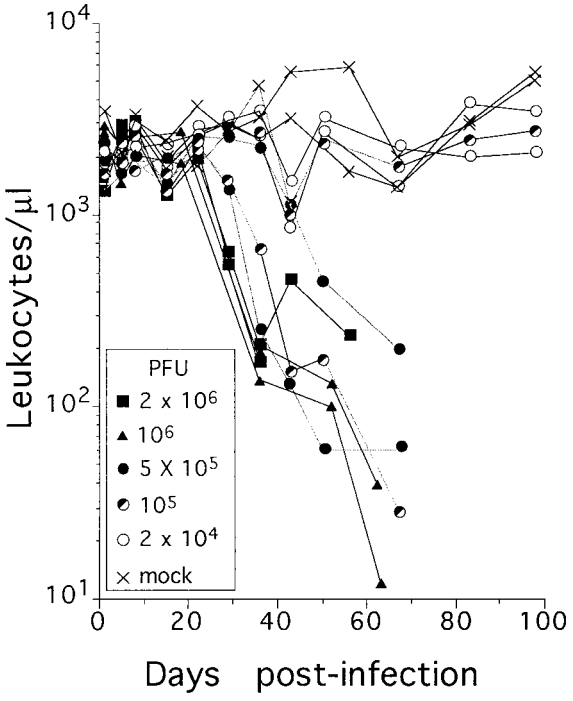

FIG. 1. Kinetics of peripheral blood leukocytes in MVMi-infected SCID mice. Each point represents the leukocyte counts determined in a single mouse. The data are from two representative mice per viral dose analyzed over the surviving time. The endpoints of the interrupted curves before day 100 indicate the day of death of the animals.

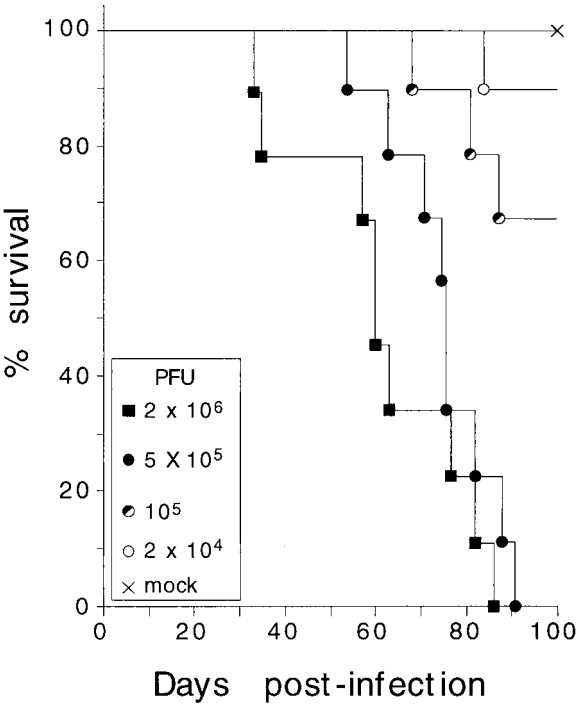

FIG. 2. Dose-dependent mortality of SCID mice after intranasal inoculation of MVMi. Each point represents the survival rate obtained from the analysis of 10 SCID mice per viral dose for a 100-day period. Comparable results were obtained from two independent experiments. Data were scored twice daily.

ELITE ESP flow cytometer (Coulter, Hialeah, Fla.). Viable cells were gated by forward and side scatter of light.

Southern analysis of viral DNA. At the indicated days, 10^6 bone marrow cells from infected mice were pelleted, and MVMi replicative intermediates were purified by a modified Hirt procedure with carrier tRNA to ensure quantitative yields as previously described (51). DNA was fractionated by agarose gel electrophoresis, blotted to nylon membranes (GeneScreen Plus; Dupont-NEN) by capillary transfer, and hybridized with MVM DNA gel-purified from a recombinant clone containing the entire virus genome (53). The probe was labeled by random priming to a specific activity of 10^9 cpm/μg and hybridized overnight at 42°C in 50% formamide, 5× SSC (1× SSC is 0.15 M NaCl plus 0.015 M sodium citrate), 5× Denhardt solution, 10% dextran sulfate (Pharmacia), 1% sodium dodecyl sulfate (SDS), and 200 μg of denatured salmon sperm DNA per ml. A final washing of the filters was done at 56°C in 0.1× SSC–0.5% SDS. Kodak X-Omat films were exposed to the filters with an intensifying screen at −70°C.

RESULTS

Parvovirus MVMi infection causes leukopenia and death in SCID mice. As a preliminary study to evaluate the capacity of MVMi to affect adult SCID mouse hemopoiesis by the natural route of infection, mice were intranasally inoculated with graded doses of purified MVMi and monitored for the level of peripheral blood leukocytes for 100 days. A progressive and dose-dependent reduction in the number of leukocytes was observed in the infected mice (Fig. 1). By 1 month postinoculation, animals inoculated with doses of 5×10^5 PFU or higher developed an acute progressive leukopenia that reduced leukocyte numbers below 200 WBC/μl prior to death. Six of eleven mice inoculated with 10^5 PFU also developed severe leukopenia and had a fatal course (Fig. 1 shows two examples of this dose), while animals inoculated with 2×10^4 PFU did not show disease.

The fact that no mouse with progressive leukopenia survived suggested the involvement of the hemopoietic system in the death of the mice. To explore this further, the mortality of the animals at these viral doses was studied. Figure 2 depicts a survival curve obtained from 10 mice per inoculated dose. Mortality in MVMi-infected SCID mice was clearly dose dependent, reaching 100% in the mice inoculated with a dose of 5×10^5 or higher. These animals showed evident pathological signs as ruffled fur and hunched posture by 40 days postinfection (d.p.i.), and these symptoms were exacerbated when the animals became moribund. At 10^5 PFU the mortality was close to 30%, a dose at which only a fraction of the mice developed leukopenia (see Fig. 1). A clear effect of the viral dose on the survival time of the mice was also noted, as the first deaths for the 2×10^6-PFU dose occurred by 35 d.p.i., by 60 d.p.i. for the 5×10^5-PFU dose, and as late as 90 d.p.i. for the 2×10^4-PFU dose. No deaths occurred after 90 d.p.i., regardless of the MVMi inoculum size. In order to assure consistent results, the uniformly lethal dose of 10^6 PFU per mouse was taken for the subsequent experiments.

A very severe leukopenia but no anemia develops in SCID mice infected by MVMi. To analyze the complete hematological pattern of the MVMi induced disease, the blood cells of a large series of infected SCID mice were quantitatively and morphologically studied. Individual animals inoculated with a lethal dose of 10^6 PFU were sacrificed and analyzed at different times postinfection. An acute leukopenia defined by a two-logarithmic-unit reduction in the leukocyte numbers developed with a 100% incidence in the inoculated mice (Fig. 3A). Moreover, both the time of onset by 25 d.p.i. and the course obtained for the whole group of mice faithfully reproduced the results noted in a single monitored mouse (Fig. 1), highlighting the reproducible character of the severe leukopenia. Remarkably, no significant changes in the number of platelets or erythrocytes were noted during the survival period of any of the leukopenic animals (Fig. 3A). This indicated that

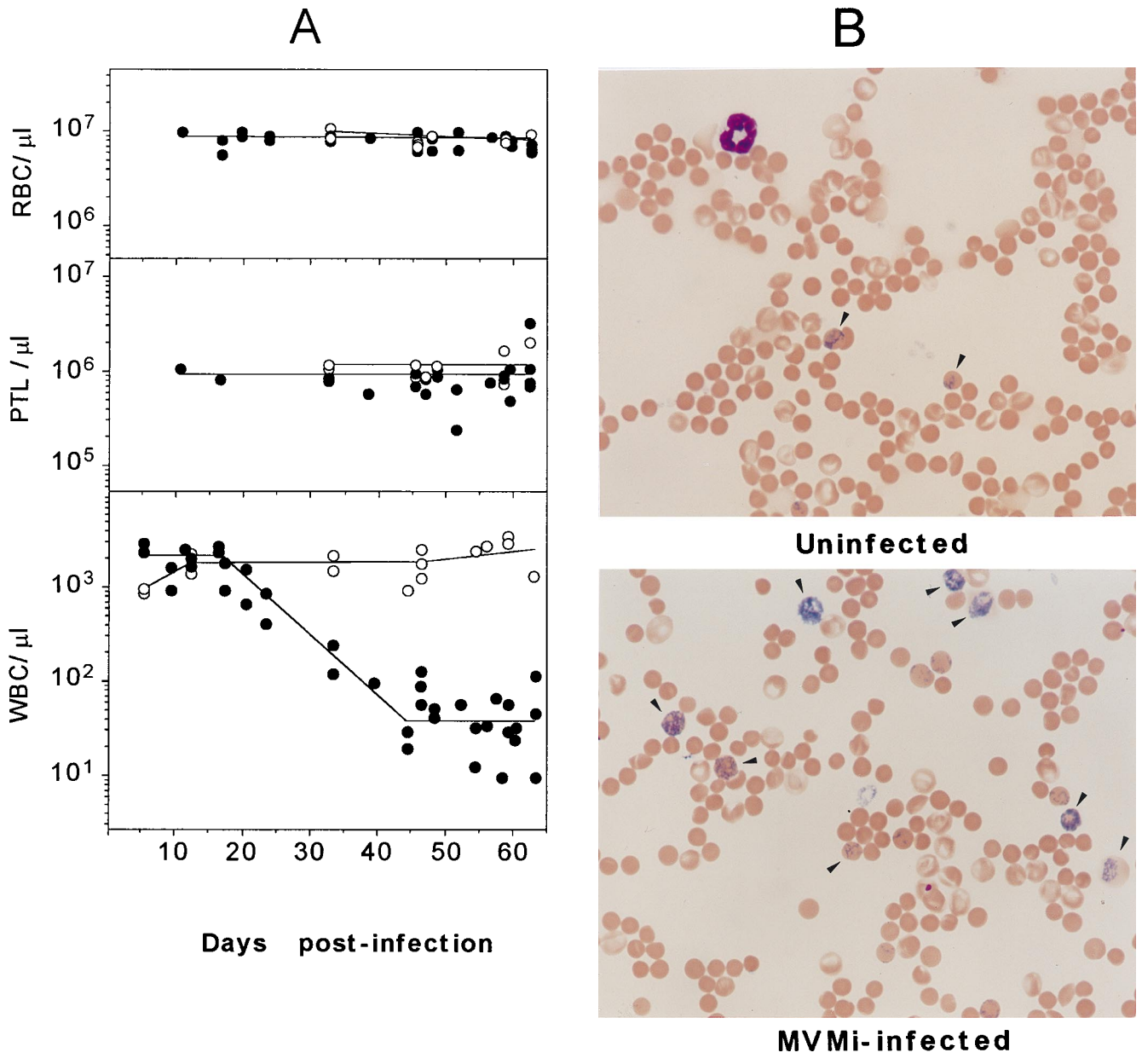

FIG. 3. Blood analysis of SCID mice. (A) Peripheral blood cell counts. The number of peripheral blood erythrocytes (RBC), platelets (PTL), and WBC are shown for mock-infected mice (○) and for mice intranasally inoculated with a lethal dose of 10^6 PFU of MVMi (●). Each point represents the data obtained from one mouse sacrificed at the indicated time postinoculation. Curves were fitted manually. Note the severity of the granulocytopenia induced by the infection. (B) Induction of reticulocytosis in MVMi-infected SCID mice. The figure illustrates blood smears from a control (uninfected) mouse and from a mouse inoculated with 10^6 PFU of MVMi at 45 d.p.i. Smears were stained with Cresil Blue to show reticulocytes (arrowheads) and counterstained with May-Grünwald-Giemsa. Magnification, ×400.

the suppressive effect of MVMi infection on mature blood cells was lineage restricted.

When the peripheral blood films of mice at 40 d.p.i. and beyond were examined, other aspects of the hemopathology of MVMi infection were manifested. First, the very few leukocytes remaining showed no relative enrichment for neutrophils, basophils, or eosinophils. In addition, the blood films also revealed that while no morphological changes in the mature erythrocytes were apparent, the proportion of reticulocytes rose from 1.5 ± 0.3% in the uninfected mice to an average of 6.5 ± 2% in the infected population (n = 5), results irrespective of the 40- to 60-d.p.i. interval of analysis taken (see Fig. 3B for a 45-d.p.i. example). These studies were further complemented with quantitative hematological analyses performed with leukopenic mice (<200 WBC/μl) at 40 to 60 d.p.i. (see Table 1). Erythroid indices that reflect erythrocyte functionality, such as hemoglobin concentration, mean corpuscular volume, etc., remained unchanged in the infected mice with respect to the control values, and only a mild decrease in the erythrocyte counts and the hemoglobin concentration were denoted (Table 1). Thus, although the infected mice did not become anemic even in the face of a very severe leukopenia, the significant reticulocytosis suggested an underlying alteration in the definitive erythropoiesis.

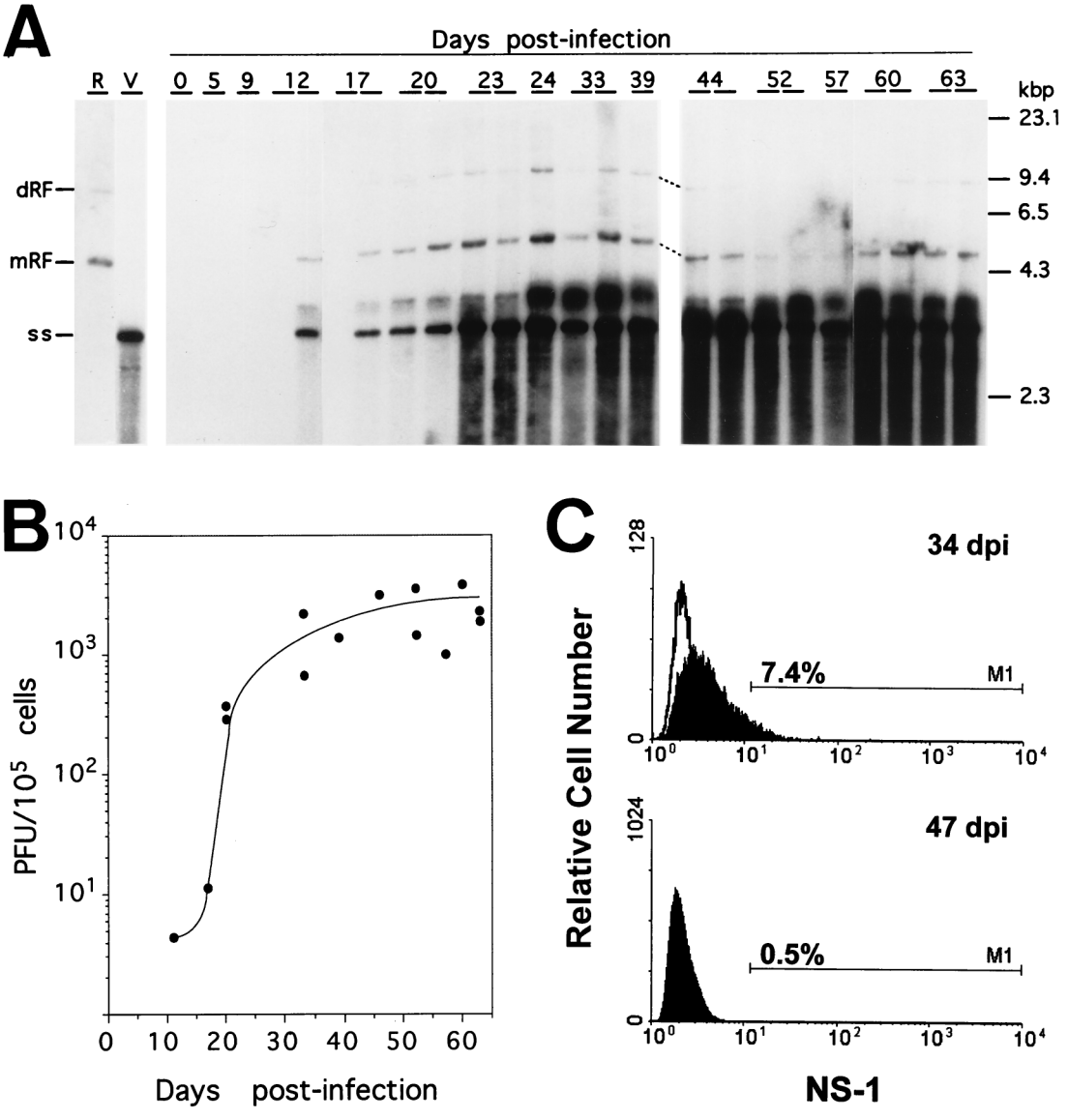

FIG. 4. Analyses of MVMi multiplication in the bone marrow of SCID mice. (A) Southern blot of MVMi DNA. Duplicate mice independently inoculated in two experiments were analyzed at each time point. Each gel slot was loaded with low-molecular-weight DNA obtained from 8×10^4 bone marrow cells. Blots were hybridized as described in Materials and Methods and exposed 40 h for autoradiography. The positions of the molecular weight standards, as well as of the viral genomic (ss) and replicative forms (mRF and dRF) are indicated. R, replicative intermediate markers from MVMi-infected EL-4 cells; V, MVMi genomes isolated from purified virions. (B) Infectious MVMi particles in the SCID bone marrow. Bone marrow suspensions were homogenated by three cycles of freeze-thawing and clarified by centrifugation, and the infectious virus content was determined in duplicate by plaque assay. Each point represents the titer obtained from one individually analyzed mouse. (C) FACS analysis of MVMi NS-1 protein expression. The fluorescence obtained with an anti-NS1 monoclonal reacting with the bone marrow cells of uninfected controls (open curves) and two SCID mice at 34 and 47 d.p.i. (filled curves) is shown. The percentages of the cells showing fluorescence values above the gated background are indicated.

MVMi multiplies in the bone marrow of SCID mice during a definite postinfection interval but persists in this organ for life. In order to investigate whether the onset and the course of the leukopenia could be explained by virally induced marrow damage, we studied the kinetics of viral DNA replication and virus production in the bone marrow after intranasal infection. Viral replicative (mRF and dRF) and genomic (ss) DNA forms were detected as early as 12 d.p.i. in the bone marrow (Fig. 4A), and after 17 d.p.i. they prevailed for life in the whole collection of animals tested. It is noteworthy that the relative level of replicative intermediate forms was highest from 20 to 40 d.p.i., indicating the time period at which viral multiplication was maximal in this organ. A general smear of low-molecular-weight viral DNA was evidenced in all of the marrows harvested from 23 d.p.i., a phenomenon not seen in either primary hemopoietic cultures (53) or in newborn mice infected by MVMi (54) but which was previously described in other persistent infections with parvoviruses (7, 26, 29). The signal from the smears cannot be accounted for from just the pool of replicative intermediate molecules accumulated by the mice at 20 d.p.i., and therefore a continuous turnover of DNA synthesis and degradation at a low rate during the course of the disease presumably occurs. The blot analysis also illustrated a higher ratio of genomic ssDNA to mRF with respect to the

values commonly found in permissive cell lines in vitro (20). This pattern is similar to that seen in adult minks persistently infected by ADV (7) and may likewise correspond to the sequestration of virion particles by marrow phagocytes (8).

In agreement with the accumulation of viral DNA, infectious MVMi particles denoted by a plaque formation assay (see Materials and Methods) were reliably detected in the marrow samples (Fig. 4B). Infectious virus appeared at detectable levels by 12 d.p.i. and rose more than 100-fold in the 20- to 35-d.p.i. interval, a finding paralleling the times for maximal MVMi DNA replication. However, the virus did not multiply unrestricted in the marrow, since the yield of infectious virus particles reached a plateau in the range of just 1×10^3 to 3×10^3 PFU/10^5 cells. This virus level persisted for the lifetime of the animals, as did the level of viral DNA demonstrated in the blots. Thus, these analyses demonstrated a burst of MVMi multiplication at the 20- to 40-d.p.i. interval; infectious virus, however, showed a noticeable capacity to persist in the marrow until the death of the mice.

The MVMi productive infection occurs in a small subset of SCID marrow cells and correlates temporarily with a deep suppression of granulomacrophage and erythroid committed progenitors. The mechanisms underlying the leukopenia induced by MVMi was next investigated by determining the number of virus-infected cells and the functionality of the hemopoiesis that takes place primarily in the bone marrow in the adult mouse. To address the question of which cells were targets for productive MVMi infection, we traced the expression in the bone marrow of the main replicative MVMi polypeptide, namely, the nonstructural NS-1 protein. Marrow cells from mice at different times postinfection were reacted with a mouse monoclonal antibody raised against NS-1 and then analyzed by flow cytometry. Illustrative results for mice at 34 and 47 d.p.i. are shown in Fig. 4C. NS-1 expression was undetectable prior to 20 d.p.i., reached a maximum at around 35 d.p.i., and was decreased in marrow sampled beyond 40 d.p.i.. This time course of NS-1 expression matches the timing of the other MVMi multiplication parameters (Fig. 4A and B). However, the number of productively infected bone marrow cells was always low regardless of the time of analysis, and even at the height of the disease the level never exceeded 8% of the population. This result was further supported by immunofluorescence analysis of Cytospin bone marrow samples reacted with an MVM capsid antiserum (51), an analysis which showed scarce positively stained cells mainly in the 30- to 40-d.p.i. interval (data not shown). Importantly, the cells positive for NS-1 labeling were negative for the differentiation markers used in the fluorescence-activated cell sorter (FACS) analysis (see below); consequently, this left the assignment of the precise target cells unresolved. We can conclude, however, that the MVMi multiplies and matures in a small population of undifferentiated cells preferentially around 35 d.p.i. At a later time, the bulk of permissive target cells may be limiting, although a basal viral multiplication seemed to occur throughout the lifetime of the infected animals.

The functionality of the SCID mice hemopoietic system was monitored by measuring the cellularity (as vital, stained cells), as well as the content of BFU-E and CFU-GM hemopoietic committed progenitors in clonogenic assays. The femoral cellularity showed a progressive reduction after 35 d.p.i. (Fig. 5, upper panel) declining to 20% of the control values at later times. The population of primitive progenitors of the erythroid lineage (BFU-E) was abruptly depleted in the infected animals after 20 d.p.i. by a factor of 20- to 50-fold with respect to the controls (Fig. 5, middle panel). The number of CFU-GM progenitors also declined along a similar course (Fig. 5, bottom panel), beginning by the time the leukopenia began (see Fig. 1). The fact that the deep depletion of hemopoietic progenitors occurred during the 20- to 35-d.p.i. interval, the main period of time for virus multiplication (see Fig. 4), strongly suggested that the two phenomena were directly connected. On the contrary, the finding that the reduction in the total number of viable cells only happened from 35 d.p.i. onwards, once the viral multiplication has declined, suggested this is not being directly related to virus infection.

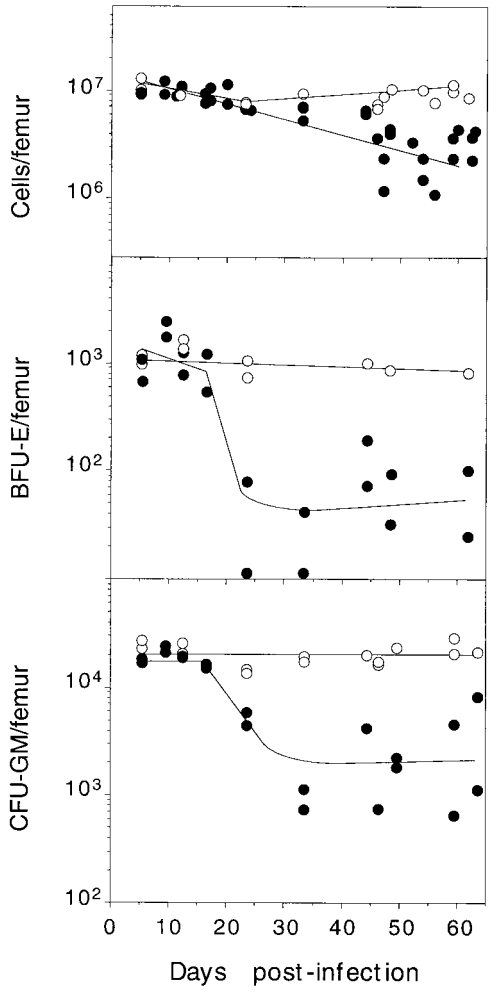

FIG. 5. Followup of hemopoietic committed progenitors in SCID bone marrow during the course of MVMi-induced disease. The figure illustrates the total number of viable nucleated cells and the BFU-E and CFU-GM clonogenic progenitors per femoral bone marrow of mock-infected mice (○) and mice infected with 10^6 PFU of MVMi (●). Each point represents the data obtained from one individually analyzed mouse. Approximate curves were fitted manually.

MVMi-infected SCID bone marrow lacks myelopoiesis and displays an erythroid hyperplasia with quantitative apoptosis. The marked reduction in the number of BFU-E progenitors in the bone marrow of the infected mice was surprising because the erythroid indices in the peripheral blood were essentially normal throughout the survival time (Table 1). To explore the mechanism of this striking inconsistency, flow cytometry analysis of the bone marrow was conducted in animals beyond 45 d.p.i. that displayed the chronic hematopoietic syndrome. This study revealed that a large fraction of the cells in the infected marrow were undergoing apoptosis. In the representative example of a 55-d.p.i. mouse outlined in Fig. 6, 30.9% of

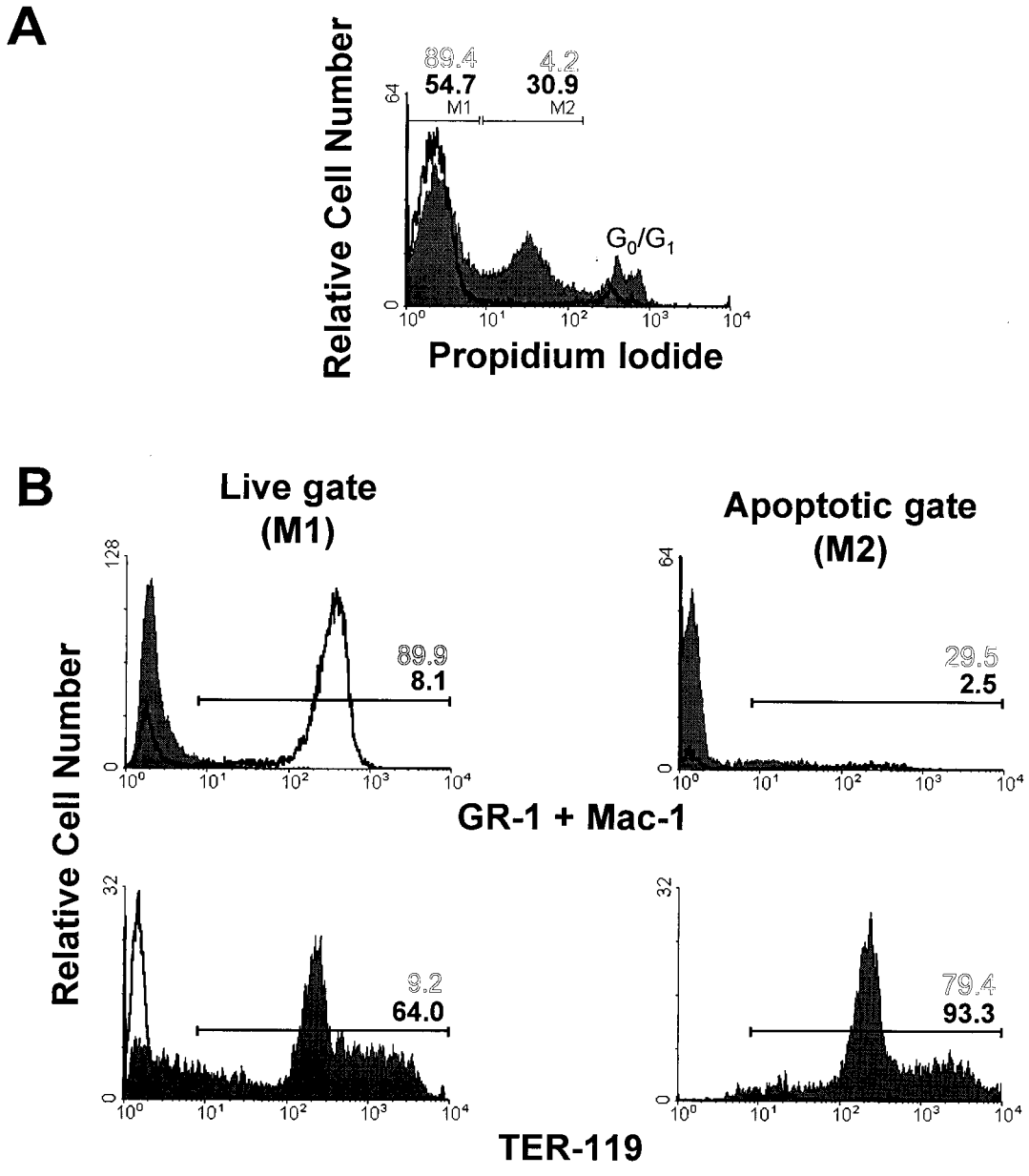

FIG. 6. Phenotypic features of MVMi-infected SCID bone marrow. Bone marrow cells harvested from uninfected (open plots) and from a representative mouse at 55 d.p.i. inoculated with 10^6 PFU of MVMi (filled plots) were labeled with the indicated monoclonal antibodies, stained with PI, and subjected to FACS analysis. (A) Total bone marrow cells electronically gated by PI uptake. The gates were set to discriminate viable cells that did not fluoresce (gate M1) from apoptotic cells fluorescing more brightly (gate M2). The low proportion of death cells showing high PI staining and normal DNA content (G_0/G_1 region) were not considered in the analysis. (B) Phenotypic analysis of the live and apoptotic gates. Positive regions were selected by staining the cells with control isotypic antibodies. Numbers represent the percentage of positive cells in the indicated regions from the uninfected (open numbers) and the infected (solid numbers) marrow samples.

the cells in the infected marrow showed evidence of apoptosis versus the normal low value of 4.2% in the uninfected mouse population (Fig. 6A, gate M2). Remarkably, 93% of the apoptotic cells of the infected marrow showed a high fluorescence value for the TER-119 marker (Fig. 6B, bottom right panel), a clear indication that this process of programmed cell death was specifically affecting precursors at definitive differentiation stages in the erythroid lineage. On the other hand, the phenotypic analysis of the remaining live cells in the samples (Fig. 6, gate M1) exhibited a >10-fold depletion (from 89.9 to 8.1%) of myeloid cells stained with GR-1 and MAC-1 antibodies in the infected bone marrow (Fig. 6B, left panels), while the proportion of erythroid TER-119^+ cells (Fig. 6B, bottom left panel) increased up to 7-fold (from 9.2 to 64%) with respect to the percentage of viable cells in the uninfected marrow. This analysis, performed in several animals, consistently demonstrated that the bone marrow hemopoiesis of the infected SCID mice shifted to an erythrocyte hyperplasia in the advanced course of the disease.

A stressed definitive erythropoiesis with proerythroblastic hyperplasia follows the MVMi-induced marrow damage. In order to determine the functionality in differentiation terms of the erythrocytes accumulated in the marrow of the infected mice, Cytospin bone marrow samples were subjected to cyto-

logical examination. In agreement with the flow cytometry analyses, samples harvested at 48 d.p.i. and beyond depicted a virtual absence of myeloid elements of either blastic or mature granulocytes (Fig. 7B), which are the most common elements in the uninfected marrow (Fig. 7A). In contrast to the absence of granulopoiesis, erythroid forms were easily recognizable in the infected bone marrows (Fig. 7B), and the May-Grünwald-Giemsa staining allowed us to morphologically classify and quantitate the proportion of erythroid precursors at specific differentiation stages (Fig. 7C). The analysis demonstrated that the high relative enrichment of erythrocytes in the infected marrow was actually only 2.3-fold the level of uninfected marrow if the absolute number of cells per femur is considered (total RBC in Fig. 7C). This expansion of the erythroid pool corresponded to an increase in the number of mitotic figures that raised the mitotic index from 0.27 ± 0.11 in the control samples to 2.8 ± 0.31 in the marrow of infected mice ($n = 4$; data not shown). Interestingly, all of the precursors of the erythroid spectrum were quantitatively represented; thus, the infection did not impose a blockade onto the differentiation potential of this hemopoietic lineage. However, while basophilic erythroblasts and the later stages of differentiation polychromatic and orthochomatic erythroblasts were represented in the infected samples in the range of the 2-fold enrichment found for the whole-cell population, the pool of proerythroblasts was increased by a significant 12-fold factor (Fig. 7C). Altogether, these analyses demonstrated that even if all of the morphologically characterized erythroid precursors contributed to the hyperplasia developing in the advanced course of the disease, the overrepresentation of the most immature proerythroblasts indicated that uneven proliferative stimuli were being exerted across the definitive erythropoiesis of the infected mice.

DISCUSSION

We have analyzed here the hematological disease caused by the parvovirus MVMi in an immunodeficient model of its natural host. The adult SCID mice allowed us to explore the tropism of the virus for hemopoietic cells in vivo in the absence of specific immune responses that cleared the virus quickly (54) and avoiding the diverse pathologies arising in the developing organs of newborn mice (14, 51). In fact, we found that the MVMi multiplied and persisted for weeks in the bone marrow of C.B-17 SCID mice, inducing a chronic hematological disease without the renal and neuropathologies found in the acute infection of BALB/c newborn mice that led to death within 10 days (14, 51). Remarkably, every mouse inoculated via the oronasal cavity with a dose of 5×10^5 PFU or higher developed a severe leukopenia with a similar course (Fig. 1) and died within 100 days (Fig. 2). The reliable capacity of the MVMi to spread from a natural oronasal infection to the distal organs of the adult mouse and to produce a lethal disease targeting hemopoietic cells indicates that hemopoietic tropism is a major property of MVMi biology and of its virulence for its host.

To understand the cellular basis of the disease, we addressed the identification of the hemopoietic cells infected by the virus. The parameters used to monitor MVMi in the SCID bone marrow, including viral DNA replication, infectious particle yields, and the percentages of productively infected cells expressing the NS-1 major replicative antigen (Fig. 4), indicated that the virus multiplies in the marrow mainly in the 20- to 35-d.p.i. interval. This time period strictly correlated with the depletion of CFU-GM and BFU-E committed progenitors (Fig. 5), strongly suggesting that the MVMi productively and cytotoxically infects this hemopoietic compartment. In addition, this may explain why MVMi multiplication reached a plateau even in the absence of a specific immune response (Fig. 4) as the number of available progenitors drops. This conclusion is in agreement with the previously described susceptibility of these cells to the virus in vitro (53) and was further strengthened by the finding that the percentage of positive cells for anti-MVM capsid immunofluorescence or NS-1$^+$ cells by FACS analysis was always low, while those stained cells were negative for the TER-119 and GR-1 differentiation markers (data not shown). Altogether, these observations support the notion that the erythroid and granulomacrophage CFU progenitors are the direct target of the MVMi infection in vivo. Moreover, the maintenance of an effective definitive erythropoiesis in the face of persistent virus multiplication indicates that the virus is most likely unable to infect maturing erythropoietic cells. It may therefore be suggested that the MVMi hemopoietic receptor(s) is restricted to primitive progenitors, including members of the multipotential compartment (CFU-S [53]), as well as of the committed compartment (CFU-GM and BFU-E), and that most probably its expression is downmodulated with differentiation. These results discriminate the MVMi hemopoietic susceptible cells from those of the B19, the only known human pathogenic parvovirus. In the latter case, the main target cells expressing the P-antigen B19 receptor (13) are exclusively of the erythroid lineage (44) and, in contrast to the MVMi findings, the susceptibility to B19 infection increases with the level of erythroid differentiation (60).

The hallmark of the hematopathology caused by MVMi infection in the SCID mice is a profound and lasting unbalance of the hemopoiesis and is characterized by a very severe leukopenia and the preservation of the erythroid indices throughout the course of the disease. In other words, the level of circulating erythrocytes, the hematocrit, and the hemoglobin content were essentially normal (Table 1), although the reticulocyte count was elevated. The leukopenia is most probably caused by the viral suppression of marrow myeloid progenitors, as revealed by the clonogenic assays (Fig. 5) and the cytological analysis (Fig. 7). But the fact that, under an equivalent depletion of committed progenitors of both lineages (CFU-GM and BFU-E), erythropoiesis recovers while granulopoiesis does not is a unique and interesting phenomenon that deserves comprehensive study. It seems unlikely that permissiveness to MVMi infection is more favored in maturing myeloid cells than in the respective erythroid ones because there is a low number of productively infected marrow cells at any time in the course of the disease (measured by NS-1 and capsid protein expression) compared with the relative abundance of myeloid precursors in the bone marrow. Therefore, a clue to the phenomenon may lie in an inherent and specific capacity of the erythropoiesis to compensate for the viral suppression of primitive progenitors.

Several parameters do indicate an important stress occurring along the erythroid lineage. In the infected marrows, although the whole pattern of erythroid differentiation was represented, there was an absolute enrichment of erythrocytes per femur that reached as much as 12-fold for the proerythroblast forms (Fig. 7C). This proerythroblastosis is most remarkable given the 50-fold absolute reduction in the number of the earlier BFU-E erythroid progenitors and, as such, is a clear indication of the stress exerted during the BFU-E/proerythroblast transition to compensate for the viral suppression of primitive progenitors. Therefore, the few BFU-E escaping the infection must be recruited for erythropoiesis through a pathway of proliferation and differentiation at a higher rate than

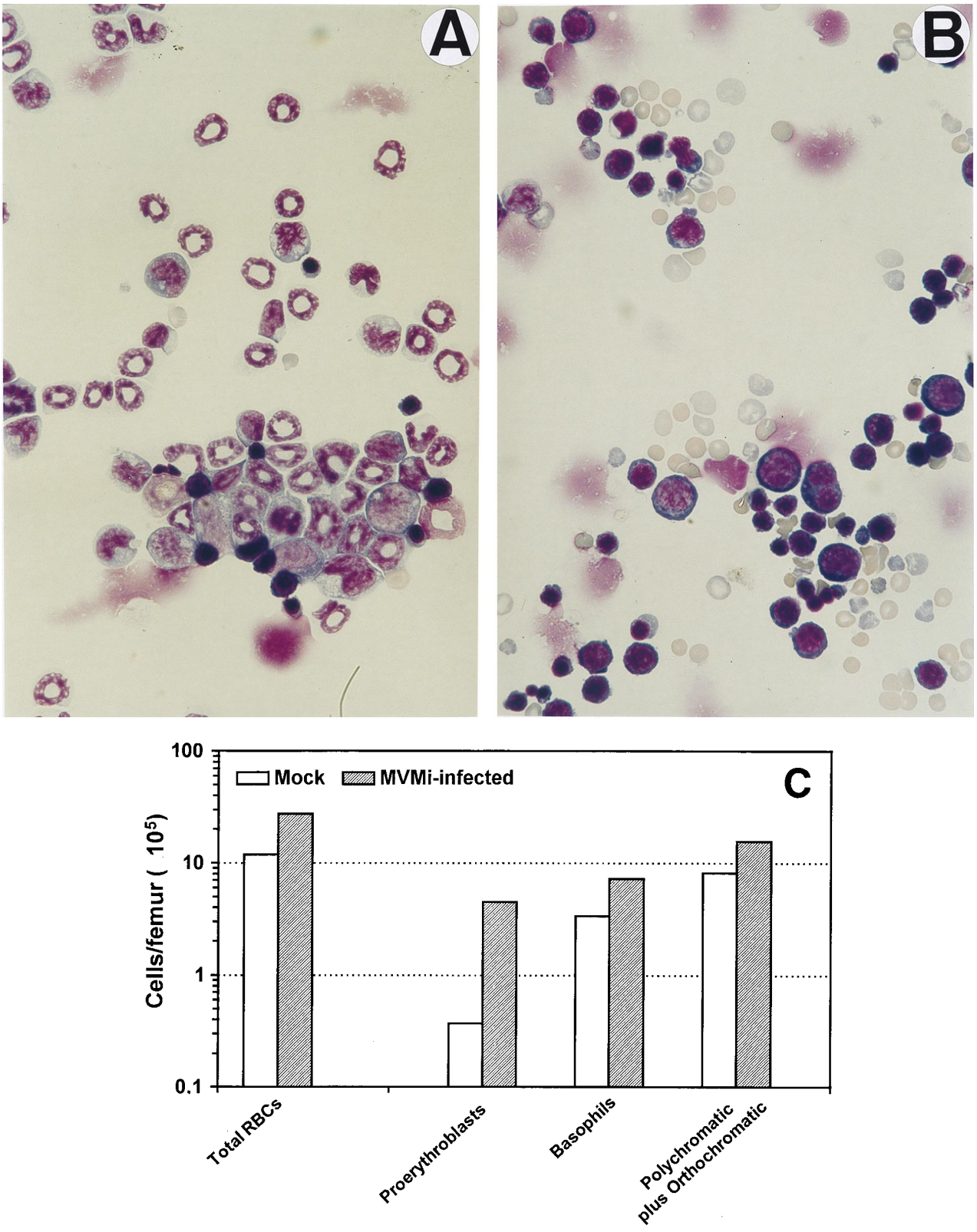

FIG. 7. Morphology and erythroid differentiation of SCID bone marrow cells. Microphotographs show May-Grünwald-Giemsa stains of Cytospin preparations of bone marrow cells harvested from uninfected mice (A) and from a mouse inoculated with 10^6 PFU of MVMi 48 days prior to analysis (B). Myeloid precursors and mature granulocytes are exclusively seen in the uninfected sample, and erythropoietic cells are predominant in the infected marrow. Magnification, ×640. (C) The figure shows the differentiation spectrum of erythroid cells in the bone marrow of mock- and MVMi-infected SCID mice. Each bar is the average of two independent experiments. The values were obtained from several visual fields, and at least 200 cells were counted for each precursor type.

normal in order to generate a large number of proerythroblasts. This precursor, with a high proliferative potential and a producer of hemoglobin (25) and which is probably less susceptible to the virus (see above), would then continue its development stimulated by the crucial action of erythropoietin (68). Experiments are underway to test this hypothesis. Clear manifestations of this developmental stress across the definitive erythropoiesis of the infected SCID mice were the increased mitotic index and the quantitative apoptosis in the TER-119$^+$ erythroid cells (Fig. 6). The latter phenomenon begins late in the survival time of the mice (from 40 d.p.i.), when the virus multiplication level has reached a plateau (Fig. 4) and the number of total viable marrow cells has begun to decline (Fig. 5, upper panel). The lack of correlation with the timing of virus multiplication in the marrow suggests that the apoptosis is neither related to the direct viral infection nor related to the cytotoxic capacity demonstrated for the NS-1 protein of MVM (15, 37). Moreover, the fact that it did happen in a highly significant proportion of erythroid TER-119$^+$ cells (Fig. 6), which were uninfected according to both NS-1 and capsid antigen expression, further strengthens this conclusion. Rather, such an apoptotic pattern is most likely due to alterations resulting from the nonphysiological virally triggered stress in the synthesis or balanced activity of the critical growth factors required for the proliferation, differentiation, and survival of hemopoietic cells (30, 55, 66, 67). Finally, the fourfold reticulocytosis due to a premature egress of reticulocytes from the marrow could be manifestation of a space requirement (38), an idea consistent with the expansion observed in the marrow and the above-mentioned stress.

Much remains to be learned about the pattern of cytokine action that upregulates the erythropoiesis in MVMi-infected SCID mice. The study of erythropoiesis in MVM infections may shed light about the normal responses of progenitor cell pools to feedback signals of hemopoiesis control, as well as about the pathogenesis of other hemopoietic diseases. Interestingly, several parvoviruses also cause diseases whose pathogenesis is not simply explained by the viral infection of the target cells. The Kilham rat virus induces acute type I diabetes in rats, infecting lymphoid tissues but not pancreatic beta cells (12), and the macrophage-derived cytokines seems to play a critical role in this autoimmune diabetes (18). The B19-associated rheumatoid arthritis (19) may be associated with a deregulated interleukin-6 (IL-6) expression in response to induction by the NS-1 protein (41), leading to endothelial cell proliferation and the polyclonal activation of B cells. An upregulation of IL-6 production may also underlie the immune disorder triggered by the ADV infection in minks (6). Those reports and this study highlight the complexity of establishing the molecular mechanisms of viral pathogenesis even for the genetically simple parvoviruses.

In conclusion, we describe here a novel persistent parvoviral infection in an immunodeficient adult host. The infection is characterized by dysregulation of the hemopoiesis associated with depletion of primitive progenitors, leading to a fatal leukopenia and the induction of compensatory mechanisms in the erythroid lineage. This reliable MVMi-SCID model system should be useful for studying the role of immune cellular and humoral protection against parvoviruses and should provide insights for developing therapies against parvovirus infections of immunosuppressed patients (33). In addition, the MVMi infection in SCID mice may serve as a useful probe for elucidating unsuspected hemopoietic regulatory networks operating in physiological and pathological situations, particularly those connecting primitive erythropoiesis with definitive erythropoiesis.

ACKNOWLEDGMENTS

J.M.G. and J.C.S. contributed equally to this work.

We thank M. E. Bloom for critical reading of the manuscript and helpful comments; C. A. Astell for providing the NS-1 monoclonal antibody; J. S. Guilarte for stimulating discussions; S. Sanchez (RVC, London, United Kingdom) and R. M. Corot for expert study of marrow and blood films; M. Lamana for careful determinations of erythroid indices; and E. Lopez, I. Ormán, and R. Cuadros for technical assistance. We are also grateful to J. Palacín for qualified SCID mice handling.

This work was supported by research grants SAF95 02-02 and SAF95 1548-C02-01 from the Comision Interministerial de Ciencia y Tecnología (CICYT) and by an institutional grant of the Fundación Areces to the Centro de Biología Molecular "Severo Ochoa." J. M. Gallego was a fellow of the Gobierno Vasco.

REFERENCES

1. **Anderson, M. J., E. Lewis, I. M. Kidd, S. M. Hall, and B. J. Cohen.** 1984. An outbreak of erythema infectiosum associated with human parvovirus infection. J. Hyg. **93:**85–93.
2. **Anderson, M. J., P. G. Higgins, L. R. Davis, J. S. Willman, S. E. Jones, I. M. Kidd, J. R. Pattison, and D. A. J. Tyrrell.** 1985. Experimental parvovirus infection in man. J. Infect. Dis. **152:**257–265.
3. **Ansel, J. D., and G. J. Bancroft.** 1989. The biology of the SCID mutation. Immunol. Today **10:**322–325.
4. **Baldauf, A. Q., K. Willwand, E. Mumtsidu, J. P. F. Nüesch, and J. Rommelaere.** 1997. Specific initiation of replication at the right-end telomera of the closed species of minute virus of mice replicative-form DNA. J. Virol. **71:**971–980.
5. **Berns, K. I.** 1996. *Parvoviridae*: the viruses and their replication, p. 2173–2197. *In* B. N. Fields, D. M. Knipe, and P. M. Howley (ed.), Virology, 3rd ed. Lippincott-Raven Press, New York, N.Y.
6. **Bloom, M. E., H. Kanno, S. Mori, and J. B. Wolfinbarger.** 1994. Aleutian mink disease: puzzles and paradigms. Infect. Agents Dis. **3:**279–301.
7. **Bloom, M. E., R. E. Race, and J. B. Wolfinbarger.** 1987. Analysis of Aleutian disease of mink parvovirus infection using strand-specific hybridization probes. Intervirology **27:**102–111.
8. **Bloom, M. E., S. Alexandersen, S. Mori, and J. B. Wolfinbarger.** 1989. Analysis of parvovirus infections using strand-specific hybridization probes. Virus Res. **14:**1–26.
9. **Bonnard, G. D., E. K. Manders, D. A. Campbell, R. B. Herberman, and M. J. Collins.** 1976. Immunosuppressive activity of a subline of the mouse EL-4 lymphoma. J. Exp. Med. **143:**187–205.
10. **Bosma, G. C., M. Fried, R. P. Custer, A. Carroll, D. M. Gibson, and M. J. Bosma.** 1988. Evidence of functional lymphocytes in some (leaky) *scid* mice. J. Exp. Med. **167:**1016–1033.
11. **Bosma, G. C., R. P. Custer, and M. J. Bosma.** 1983. A severe combined immunodeficiency mutation in the mouse. Nature **301:**527–530.
12. **Brown, D. W., R. M. Welsh, and A. A. Like.** 1993. Infection of peripancreatic lymph nodes but not islets precedes Kilham rat virus-induced diabetes in BB/Wor rats. J. Virol. **10:**5873–5878.
13. **Brown, K. E., S. M. Anderson, and N. S. Young.** 1993. Erythrocyte P antigen: cellular receptor for B19 parvovirus. Science **262:**114–117.
14. **Brownstein, D. G., A. L. Smith, R. O. Jacoby, E. A. Johnson, G. Hansen, and P. Tattersall.** 1991. Pathogenesis of infection with a virulent allotropic variant of minute virus of mice and regulation by host genotype. Lab. Invest. **65:**357–363.
15. **Caillet-Fauquet, P., M. Perros, A. Brandenburger, P. Spegelaere, and J. Rommelaere.** 1990. Programmed killing of human cells by means of an inducible clone of parvoviral genes encoding non-structural proteins. EMBO J. **9:**2989–2995.
16. **Chipman, P. R., M. Agbandje-McKenna, S. Kajigaya, K. E. Brown, N. S. Young, T. S. Baker, and M. G. Rossmann.** 1996. Cryo-electron microscopy studies of empty capsids of human parvovirus B19 complexed with its cellular receptor. Proc. Natl. Acad. Sci. USA **93:**7502–7506.
17. **Christensen, J., S. F. Cotmore, and P. Tattersall.** 1997. A novel cellular site-specific DNA-binding protein cooperates with the viral NS1 polypeptide to initiate parvovirus DNA replication. J. Virol. **71:**1405–1416.
18. **Chung, Y. H., H. S. Jun, Y. Kang, K. Hirasawa, B. R. Lee, N. Van Rooijen, and J. W. Yoon.** 1997. Role of macrophages and macrophage-derived cytokines in the pathogenesis of Kilham rat virus-induced autoimmune diabetes in diabetes-resistant biobreeding rats. J. Immunol. **159:**466–471.
19. **Cohen, B. J., M. M. Buckllley, J. P. Clewley, V. E. Jones, A. H. Puttick, and R. K. Jacoby.** 1986. Human parvovirus infection in early rheumatoid and inflammatory arthritis. Ann. Rheum. Dis. **45:**832–838.
20. **Cornelis, J. J., P. Becquart, N. Duponchel, N. Salomé, B. L. Avalosse, M. Namba, and J. Rommelaere.** 1988. Transformation of human fibroblasts by ionizing radiation, a chemical carcinogen, or simian virus 40 correlates with an increase in susceptibility to the autonomous parvovirus H-1 virus and minute virus of mice. J. Virol. **62:**1679–1686.

21. **Cowling, G. J., and T. M. Dexter.** 1992. Erythropoietin and myeloid colony stimulating factors. Trends Biotechnol. **10:**349–357.
22. **Doerig, C., B. Hirt, J. P. Antonietti, and P. Beard.** 1990. Nonstructural protein of parvovirus B19 and minute virus of mice controls transcription. J. Virol. **64:**387–396.
23. **Doerig, C., B. Hirt, P. Beard, and J. P. Antonietti.** 1988. Minute virus of mice non-structural proteins NS-1 is necessary and sufficient for trans-activation of the viral P39 promoter. J. Gen. Virol. **69:**2563–2573.
24. **Engers, H. D., J. A. Louis, R. H. Zubler, and B. Hirt.** 1981. Inhibition of T-cell mediated functions by MVM(i), a parvovirus closely related to minute virus of mice. J. Immunol. **127:**2280–2285.
25. **Erslev, A. J.** 1990. The production of erythrocytes, p. 389–397. *In* W. J. Williams, E. Beutler, A. J. Erslev, and M. A. Lichtman (ed.), Hematology. McGraw-Hill Publishing Co., New York, N.Y.
26. **Faisst, S., S. Bartnitzke, J. R. Schlehofer, and H. zur Hausen.** 1990. Persistence of parvovirus H-1 DNA in human B- and T-lymphoma cells. Virus Res. **16:**211–224.
27. **Frickhofen, N., J. L. Abkowitz, M. Safford, M. Berry, J. Antunez-de-Mayolo, A. Astrow, R. Cohen, I. Halperin, L. King, D. Mintzer, B. Cohen, and N. S. Young.** 1990. Persistent B19 parvovirus infection in patients infected with human immunodeficiency virus type 1 (HIV-1): a treatable cause of anemia in AIDS. Ann. Intern. Med. **113:**926–933.
28. **Harris, J. W.** 1992. Parvovirus B19 for the hematologist. Am. J. Hematol. **39:**119–130.
29. **Jacoby, R. O., E. A. Johnson, F. X. Paturzo, D. J. Gaertner, J. L. Brandsma, and A. L. Smith.** 1991. Persistent rat parvovirus infection in individually housed rats. Arch. Virol. **117:**193–205.
30. **Kelley, L. L., M. J. Koury, M. C. Bondurant, S. T. Koury, S. T. Sawyer, and A. Wickrema.** 1993. Survival or death of individual proerythroblasts results from differing erythropoietin sensitivities: a mechanism for controlled rates of erythrocyte production. Blood **82:**2340–2352.
31. **Kimsey, P. B., H. D. Engers, B. Hirt, and V. Jongeneel.** 1986. Pathogenicity of fibroblast- and lymphocyte-specific variants of minute virus of mice. J. Virol. **59:**8–13.
32. **Krishan, A.** 1975. Rapid flow cytometric analysis of mammalian cell cycle by propidium iodide staining. J. Cell Biol. **66:**188–193.
33. **Kurtzman, G. J., K. Ozawa, B. Cohen, G. Hanson, R. Oseas, and N. S. Young.** 1987. Chronic bone marrow failure due to persistent B19 parvovirus infection. N. Engl. J. Med. **317:**287–294.
34. **Kurtzman, G. J., L. Platanias, L. Lustig, N. Frickhofen, and N. S. Young.** 1989. Feline parvovirus propagates in cat bone marrow cultures and inhibits hematopoietic colony formation *in vitro*. Blood **74:**71–81.
35. **Larse, S., A. Flagstad, and B. Aalbaek.** 1976. Experimental feline panleukopenia in the conventional cat. Vet. Pathol. **13:**216–240.
36. **Lawrence, J. S., J. T. Syverton, J. S. Shaw, and F. P. Smith.** 1940. Infectious feline agranulocytosis. Am. J. Pathol. **16:**333–354.
37. **Legendre, D., and J. Rommelaere.** 1992. Terminal regions of the NS-1 protein of the parvovirus minute virus of mice are involved in cytotoxicity and promoter *trans* inhibition. J. Virol. **66:**5705–5713.
38. **Lichtman, M. A., J. K. Chamberlain, and P. A. Santillo.** 1978. Factors thought to contribute to the regulation of egress of cells from marrow, p. 243–258. *In* R. Silber, J. LoBue, and A. S. Gordon (ed.), The year of hematology. Plenum Press, New York, N.Y.
39. **Metcalf, D.** 1989. The molecular control of cell division, differentiation, commitment and maturation in haemopoietic cells. Nature **339:**27–30.
40. **Miller, R. A., D. C. Ward, and F. H. Ruddle.** 1977. Embryonal carcinoma cells (and their somatic cell hybrids) are resistant to infection by the murine parvovirus MVM, which does infect other teratocarcinoma-derived cell lines. J. Cell. Physiol. **91:**393–402.
41. **Moffatt, S., N. Tanaka, K. Tada, M. Nose, M. Nakamura, O. Muraoka, T. Hirano, and K. Sugamura.** 1996. A cytotoxic nonstructural protein (NS1) of human parvovirus B19 induces the activation of interleukin-6 gene expression. J. Virol. **70:**8485–8491.
42. **Moffatt, S., N. Yaegashi, K. Tada, N. Tanaka, and K. Sugamura.** 1998. Human parvovirus B19 nonstructural (NS1) protein induces apoptosis in erythroid cells. J. Virol. **72:**3018–3028.
43. **Mori, S., J. B. Wolfinbarger, M. Miyazawa, and M. E. Bloom.** 1991. Replication of Aleutian mink disease parvovirus in lymphoid tissues of adult mink: involvement of follicular dendritic cells and macrophages. J. Virol. **65:**952–956.
44. **Mortimer, P. P., R. K. Humphries, J. G. Moore, R. H. Purcell, and N. S. Young.** 1983. A human parvovirus-like virus inhibits haemopoietic colony formation *in vitro*. Nature **302:**426–429.
45. **Owren, P. A.** 1948. Congenital hemolytic jaundice: the pathogenesis of the "hemolytic crisis." Blood **3:**231–248.
46. **Ozawa, K., G. Kurtzman, and N. Young.** 1987. Productive infection by B19 parvovirus of human erythroid bone marrow cells *in vitro*. Blood **70:**384–391.
47. **Pattison, J. R., S. E. Jones, and J. Hodgson.** 1981. Parvovirus infections and hypoplastic crises in sickle cell anaemia. Lancet **i:**664–665.
48. **Porter, D. D., A. E. Larsen, and H. G. Porter.** 1969. The pathogenesis of Aleutian disease of mink. In vivo viral replication and the host antibody response to viral antigen. J. Exp. Med. **130:**575–589.
49. **Potter, C. G., A. C. Potter, C. S. R. Hatton, H. M. Chapel, M. J. Anderson, J. R. Pattison, D. A. J. Tyrrell, P. G. Higgins, J. S. Willman, H. F. Parry, and P. M. Cotes.** 1987. Variation of erythroid and myeloid precursors in the marrow and peripheral blood of volunteer subjects infected with human parvovirus (B19). J. Clin. Invest. **79:**1486–1492.
50. **Quesenberry, P. P.** 1990. Hemopoietic stem cells, progenitor cells, and growth factors, p. 129–147. *In* W. J. Williams, E. Beutler, A. J. Erslev, and M. A. Lichtman (ed.), Hematology. McGraw-Hill Publishing Co., New York, N.Y.
51. **Ramírez, J. C., A. Fairén, and J. M. Almendral.** 1996. Parvovirus minute virus of mice strain i multiplication and pathogenesis in the newborn mouse brain are restricted to proliferative areas and to migratory cerebellar young neurons. J. Virol. **70:**8109–8116.
52. **Rhode III, S. L.** 1989. Both excision and replication of cloned autonomous parvovirus DNA require the NS1 (rep) protein. J. Virol. **63:**4249–4256.
53. **Segovia, J. C., A. Real, J. A. Bueren, and J. M. Almendral.** 1991. *In vitro* myelosuppressive effects of the parvovirus minute virus of mice (MVMi) on hematopoietic stem and committed progenitor cells. Blood **77:**980–988.
54. **Segovia, J. C., J. A. Bueren, and J. M. Almendral.** 1995. Myeloid depression follows infection of susceptible newborn mice with the parvovirus minute virus of mice (strain i). J. Virol. **69:**3229–3232.
55. **Shivdasani, R. A., and S. H. Orkin.** 1996. The transcriptional control of hematopoiesis. Blood **87:**4025–4039.
56. **Siegl, G.** 1988. Patterns of parvovirus disease in animals, p. 43–67. *In* J. R. Pattison (ed.), Parvoviruses and human disease. CRC Press, Boca Raton, Fla.
57. **Siegl, G., R. C. Bates, K. I. Berns, B. J. Carter, D. C. Kelly, E. Kurstak, and P. Tattersall.** 1985. Characteristics and taxonomy of *Parvoviridae*. Intervirology **23:**61–73.
58. **Spalholz, B. A., and P. Tattersall.** 1983. Interaction of minute virus of mice with differentiated cells: strain-dependent cell specificity is mediated by intracellular factors. J. Virol. **46:**937–943.
59. **Studdert, M. J.** 1990. Tissue tropism of parvoviruses, p. 3–27. *In* P. Tijssen (ed.), Handbook of parvoviruses, vol. II. CRC Press, Boca Raton, Fla.
60. **Takahashi, T., K. Ozawa, K. Takahashi, S. Asano, and F. Takaku.** 1990. Susceptibility of human erythropoietic cells to B19 parvovirus *in vitro* increases with differentiation. Blood **75:**603–610.
61. **Tattersall, P.** 1972. Replication of parvovirus minute virus of mice. I. Dependence of virus multiplication and plaque formation on cell growth. J. Virol. **10:**586–590.
62. **Tattersall, P., and E. M. Gardiner.** 1990. Autonomous parvovirus host-cell interactions, p. 111–121. *In* P. Tijssen (ed.), Handbook of parvoviruses, vol I. CRC Press, Boca Raton, Fla.
63. **Tennant, R. W., K. R. Laymant, and R. E. Hand, Jr.** 1969. Effect of cell physiological state on infection by rat virus. J. Virol. **4:**872–878.
64. **Toolan, H. W.** 1990. The rodent parvoviruses, p. 159–176. *In* P. Tijssen (ed.), Handbook of parvoviruses, vol II. CRC Press, Boca Raton, Fla.
65. **Török, T. J.** 1992. Parvovirus B19 and human disease. Adv. Intern. Med. **37:**431–455.
66. **Williams, G. T., C. A. Smith, E. Spooncer, T. M. Dexter, and D. R. Taylor.** 1990. Haemopoietic colony stimulating factors promote cell survival by suppressing apoptosis. Nature **343:**76–79.
67. **Wu, H., V. Klingmüller, P. Besmer, and H. Lodish.** 1995. Interaction of the erythropoietin and stem cell factor receptors. Nature **377:**242–246.
68. **Wu, H., X. Liu, R. Jaenisch, and H. F. Lodish.** 1995. Generation of committed erythroid BFU-E and CFU-E progenitors does not require erythropoietin or the erythropoietin receptor. Cell **83:**59–67.
69. **Yeung, D. E., G. W. Brown, P. Tam, R. H. Russnak, G. Wilson, I. Clark-Lewis, and C. R. Astell.** 1991. Monoclonal antibodies to the major nonstructural nuclear protein of minute virus of mice. Virology **181:**35–45.
70. **Young, N. S.** 1993. Viruses and bone marrow. Marcel Dekker, Inc., New York, N.Y.
71. **Young, N. S.** 1996. Parvoviruses, p. 2199–2220. *In* B. N. Fields, D. M. Knipe, and P. M. Howley (ed.), Virology, 3rd ed. Lippincott-Raven Press, New York, N.Y.
72. **Young, N. S., M. Yoshida, and W. Sugden.** 1992. Viral pathogenesis of hematologic disorders. *In* G. Stamatoyanapoulos, A. S. Nienhuis, P. Leder, P. Majerus, and H. Varmus (ed.), Molecular basis of blood diseases. W. B. Saunders Co., Philadelphia, Pa.